Supplementary Material

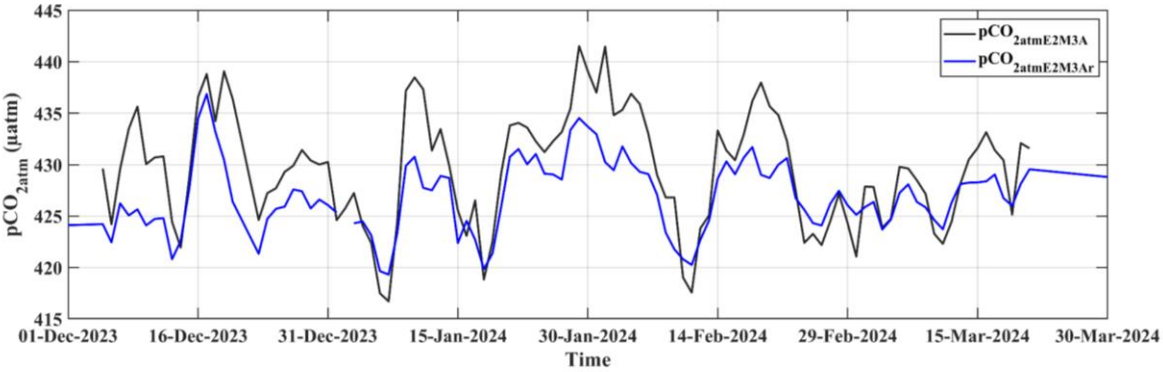

Figure S1. Time series of daily pCO_{2atm} measured at the EMSO-E2M3A (pCO_{2atm_E2M3A}, µatm) in black and the pCO_{2atm} calculated from xCO_2 from Lampedusa (pCO_{2atm_E2M3Ar}, µatm) in blue between December 2023 and March 2024. pCO_{2atm_E2M3Ar} have been calculated according to Eq. 1 and Eq. 2.

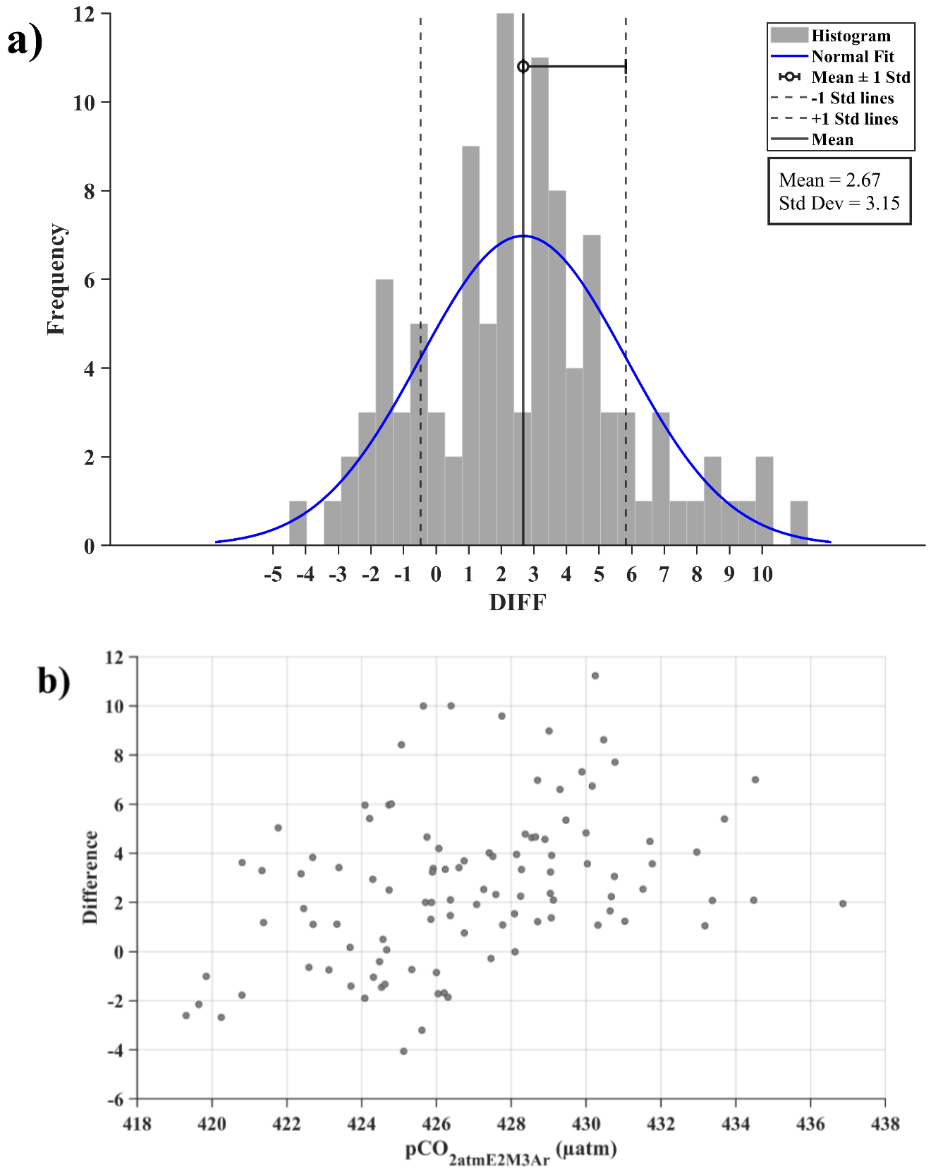

Figure S2. a) Histogram of the difference between pCO_{2atm_E2M3A} (µatm) and pCO_{2atm_E2M3Ar} (µatm) including standard deviation (Std Dev) and mean of the difference (Mean); and b) Scatterplot of the difference against pCO_{2atm_E2M3Ar} (µatm). The calculations were performed considering the data in the period from December 2023 to March 2024.

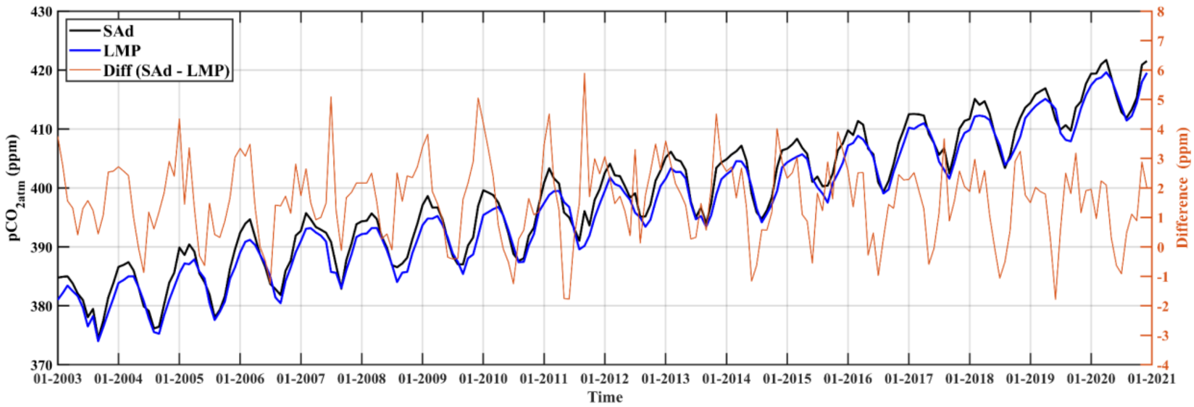

Figure S3. Monthly time series of pCO_{2atm} (ppm) at EMSO-E2M3A (SAd) and at Lampedusa (LMP) in blue and black respectively from the CAMS reanalysis of the European Centre for Medium-Range Weather Forecasts (ECMWF). The difference between the values in the two sites (SAd - LMP) is represented by the orange line.

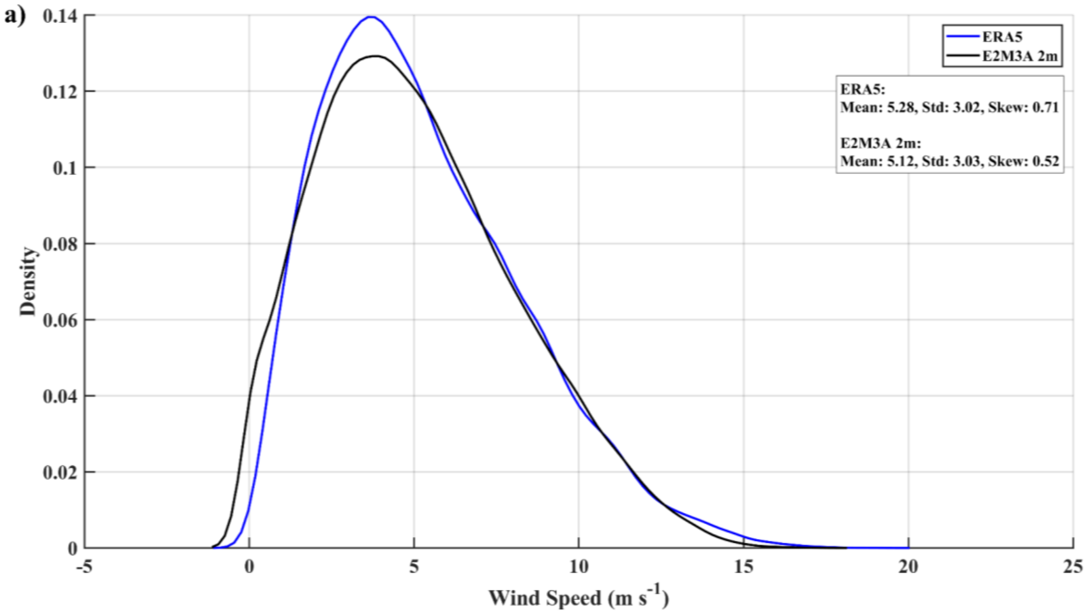

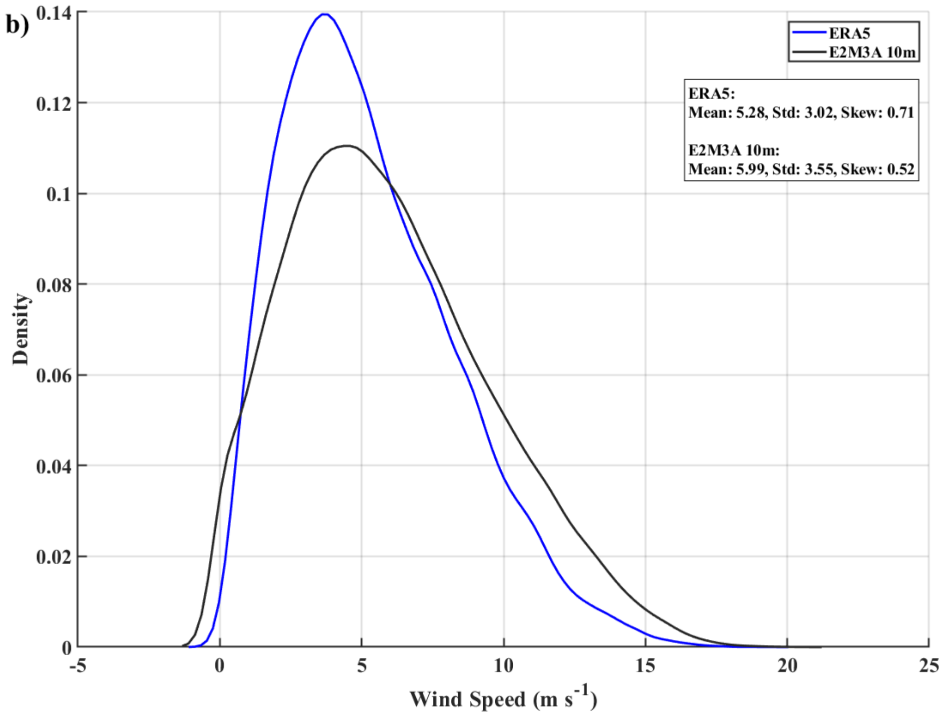

Figure S4. Distribution of a) wind speed data (m s^{-1}) measured at EMSO-E2M3A at 2 m height and from ERA5, b) Wind speed data (m s^{-1}) measured at EMSO-E2M3A at 10 m height and from ERA5. WSPD measured at EMSO-E2M3A is represented by the black curve, while WSPD from ERA5 is represented by the blue curve in both panels. The distribution refers to hourly data in the period from 2015 to 2024. For every panel, the mean difference (Mean), standard deviation (Std Dev), and skewness (Skew) is also presented.

A more detailed analysis of the different wind datasets, i.e., in situ wind speed measured at the EMSO-E2M3A observatory at 2 m height (WSPD$_{E2M3A2m}$, m s^{-1}) and the converted wind speed at 10 height (WSPD$_{E2M3A10m}$, m s^{-1}) and ERA5 (WSPD$_{ERA5}$, m s^{-1}) wind speed was performed. A better agreement was found between WSPD$_{E2M3A2m}$ and WSPD$_{ERA5}$ (mean difference of -0.16 m s^{-1}), while a higher difference of 0.71 m s^{-1} between WSPD$_{E2M3A10m}$ and WSPD$_{ERA5}$ was highlighted. Both datasets displayed considerable variability, with the largest discrepancies occurring at the distribution tails during high wind events. Specifically, ERA5 tended to report stronger winds than WSPD$_{E2M3A2m}$ for velocities > 15 m s^{-1}, whereas WSPD$_{E2M3A10m}$ exceeded ERA5 under the same conditions (Fig. S4a, S4b). In addition, ERA5 data showed greater skewness compared to in situ observations, suggesting a systematic tendency to capture with a higher frequency strong wind speed events. The differences between WSPD$_{E2M3A}$ at both heights and WSPD$_{ERA5}$ were also evaluated by classifying wind speeds according to the Beaufort scale (https://www.rmets.org/metmatters/beaufort-wind-scale), in order to assess whether discrepancies were more pronounced under specific wind conditions, particularly extreme events. The Beaufort scale, widely used in meteorology, relates mean wind speed at 10 m height to observed conditions at sea or on land, and categorizes winds into discrete intervals. When WSPD$_{E2M3A}$ and WSPD$_{ERA5}$ values did not fall exactly within these intervals, they were assigned to the closest category based on proximity to the category mean. Consistent with previous results, differences between datasets were small across most categories, but tended to increase at higher wind speeds.

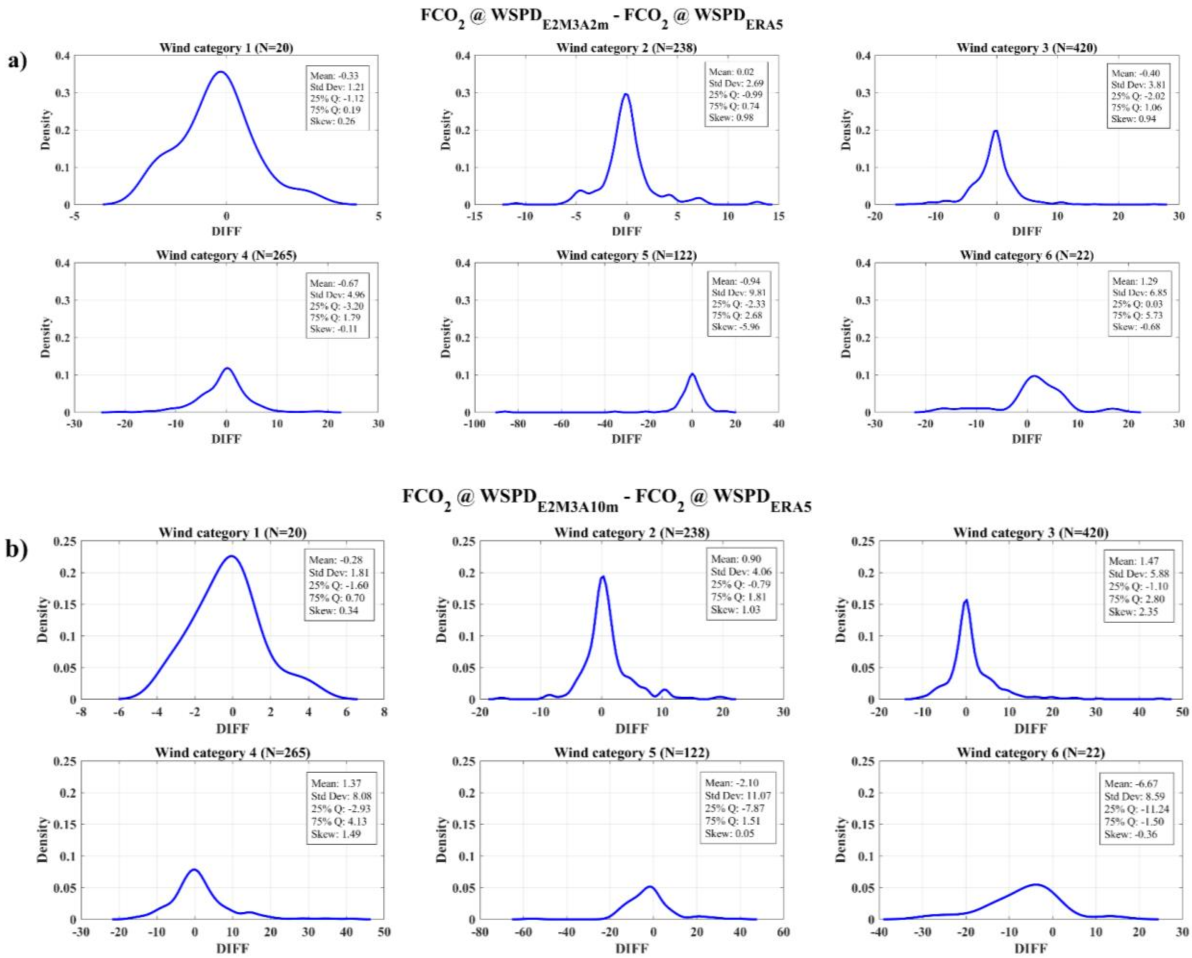

Figure S5. Distribution of the differences of CO_2 flux for each wind category defined according ERA5 wind speed between a) fluxes calculated using $WSPD_{E2M3A2m}$ (m s^{-1}) and $WSPD_{ERA5}$ (m s^{-1}) and b) CO_2 flux calculated using $WSPD_{E2M3A10m}$ (m s^{-1}) and $WSPD_{ERA5}$ (m s^{-1}). Wind categories are defined in Table 3. N refers to the number of events for each wind category in the period 2015-2024. For every panel, the mean difference (Mean), standard deviation (Std Dev), 25 % and 75 % percentile of the distribution and skewness (Skew) is also presented.

The impact on FCO_2 estimates was low within Beaufort categories between 2 and 5 (wind speed between 1.7 and 10.6 m s^{-1}), which encompass the majority of events at EMSO-E2M3A, indicating broad consistency among datasets under typical conditions (Fig. S5). However, larger discrepancies emerged at higher wind categories, especially between $WSPD_{E2M3A10m}$ and $WSPD_{ERA5}$. Both comparisons also showed substantial data dispersion, with standard deviations increasing with wind category, suggesting that variability in FCO_2 estimates derived from different wind products becomes more relevant at higher wind speeds.

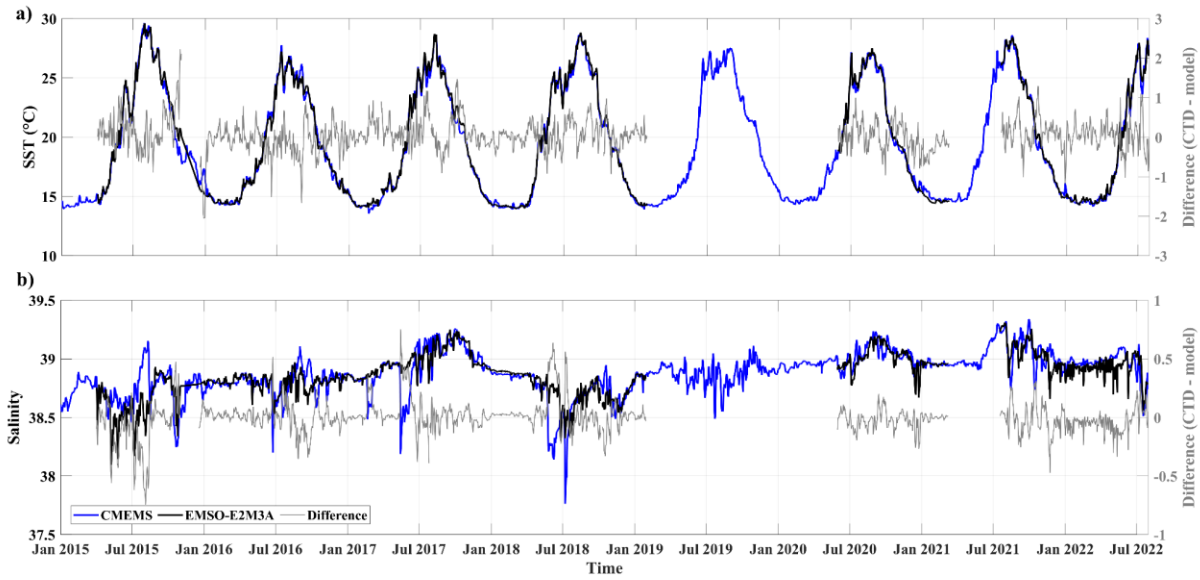

Figure S6. Comparison of daily time series of a) Sea surface temperature (SST, °C) and b) Salinity measured by the SBE ODO sensor installed on the EMSO-E2M3A regional facility and from CMEMS reanalysis in black and blue respectively. The difference between EMSO-E2M3A and model data is displayed in both panels by the grey curves.

By considering two different orders in the process of aggregating data for computing averages, the sensitivity of data sampling irregularity to the overall mean was verified. In the first approach (hereafter M1), the daily means for each day of the year were calculated. Outliners were then identified and removed through visual inspection, with particular attention to values not supported by a sufficiently large number of observations. Finally, monthly means were derived, and the overall mean for the entire study period (2015-2024) was computed from the 12 monthly averages. In the second approach (hereafter M2), a 2015-2024 time series of the monthly values is computed for those months with at least 14 valid daily values. The mean over the full period was subsequently obtained from these monthly values. A summary of the monthly means obtained with M1 and M2 is reported in Table S1.

Table S1. Monthly mean of FCO_2 (mmol m^{-2} day^{-1}) in the SAd calculated with in situ data from the EMSO-E2M3A regional facility in the period 2015-2024 using two different computation methods. Relative difference was calculated as M1 - M2 divided by M1.

Month of the year	**M1 (mmol m^{-2} day^{-1})**	**M2 (mmol m^{-2} day^{-1})**	**M1 - M2**	**Relative difference**
January	-17.92	-17.89	-0.04	0.0020
February	-16.75	-15.96	-0.78	0.0469
March	-12.79	-12.79	0.00	0.0000
April	-14.26	-11.02	-3.23	0.2269

May	6.36	9.80	-3.44	-0.5410
June	16.67	16.31	0.36	0.0215
July	22.49	21.06	1.43	0.0635
August	24.11	22.90	1.22	0.0504
September	15.61	15.58	0.03	0.0017
October	-1.99	-1.88	-0.11	0.0577
November	-15.30	-15.62	0.32	-0.0209
December	-20.14	-19.69	-0.45	0.0222

Both methods produced consistent results, with an average difference of approximately 5 % between M1 and M2. The largest discrepancies between the two methods occurred in April and May. In April these can be due to the lower data availability (Fig. 3b), as only two years of data were available. On the contrary, in May a transition between source and sink conditions occurs, thus explaining the larger differences between M1 and M2. Similarly, in February, data for only one year (2024) was available throughout the month with the addition of a few days at the beginning of February 2018 making this approach not robust enough to have reliable results (higher difference between M1 and M2). Finally, in March data were available only in 2024, and the proposed aggregating processes produced no difference between M1 and M2.